JACS
JOURNAL OF THE AMERICAN CHEMICAL SOCIETY
Article
pubs.acs.org/JACS

Reengineering the Optical Absorption Cross-Section of Photosynthetic Reaction Centers

Palash K. Dutta,[†,‡] Su Lin,[†,‡] Andrey Loskutov,[‡] Symon Levenberg,[†,‡] Daniel Jun,[§] Rafael Saer,[§] J. Thomas Beatty,[§] Yan Liu,[†,‡] Hao Yan,*[,†,‡] and Neal W. Woodbury*[,†,‡]

[†]Department of Chemistry and Biochemistry and [‡]The Biodesign Institute, Arizona State University, Tempe, Arizona 85287, United States

[§]Department of Microbiology and Immunology, University of British Columbia, Vancouver, British Columbia, V6T 1Z3, Canada

Supporting Information

ABSTRACT: Engineered cysteine residues near the primary electron donor (P) of the reaction center from the purple photosynthetic bacterium *Rhodobacter sphaeroides* were covalently conjugated to each of several dye molecules in order to explore the geometric design and spectral requirements for energy transfer between an artificial antenna system and the reaction center. An average of 2.5 fluorescent dye molecules were attached at specific locations near P. The enhanced absorbance cross-section afforded by conjugation of Alexa Fluor 660 dyes resulted in a 2.2-fold increase in the formation of reaction center charge-separated state upon intensity-limited excitation at 650 nm. The effective increase in absorbance cross-section resulting from the conjugation of two other dyes, Alexa Fluor 647 and Alexa Fluor 750, was also investigated. The key parameters that dictate the efficiency of dye-to-reaction center energy transfer and subsequent charge separation were examined using both steady-state and time-resolved fluorescence spectroscopy as well as transient absorbance spectroscopy techniques. An understanding of these parameters is an important first step toward developing more complex model light-harvesting systems integrated with reaction centers.

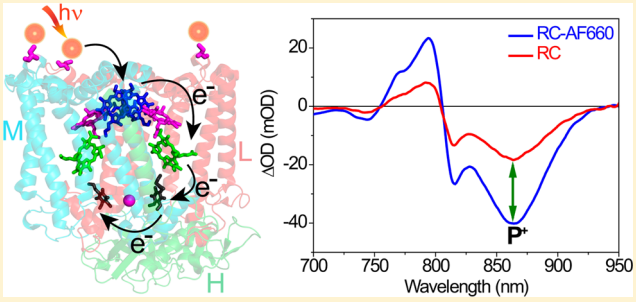

INTRODUCTION

One of the most fascinating phenomena in nature is the primary solar energy conversion event in photosynthesis.[1] Photosynthetic organisms employ a light-harvesting antenna network to collect photons and transfer their energy to the reaction center, where the energy is used to power a series of electron-transfer reactions with near unity quantum yield.[1d] The geometry and spectral properties of the light-harvesting systems used by different organisms are quite varied, depending on environmental conditions and needs.[1a] Both to further our fundamental understanding of light harvesting and to enable the engineering of artificial photonic systems, it would be useful to develop platforms in which model complexes of pigments and charge separation elements can be assembled in a spatially defined manner.

Quantum dots[2] and organic fluorophores[3] have been conjugated previously with reaction centers (RCs) and in some cases used to enhance the absorbance cross-section of the photosynthetic reaction center (RC) by absorbing light in spectral regions to the blue of the natural reaction center absorbance and then transferring energy to the reaction center initial electron donor. However, a more detailed understanding of how the specific spectral and excited-state properties of the absorbers as well as the relative geometry of the different components contribute to the overall performance of light-harvesting systems would be beneficial. Here, a genetically modified reaction center (Figure 1A) is used in conjunction with commercially available fluorescent dye molecules to

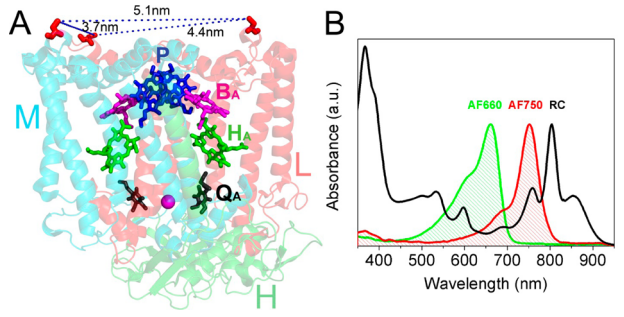

Figure 1. (A) Structure of the RC from the purple bacterium, *Rhodobacter sphaeroides* 2.4.1 (PDB 2J8C). The three protein subunits, M, L, and H and the cofactors (except carotenoid) are shown. Three unique Cys residues have been introduced (shown in red), and their relative distances are given. There are two Cys residues on the L subunit and one on the M subunit. (B) Normalized absorption spectra of the RC (black), AF660 (green), and AF750 (red). A normalized absorption spectrum of AF647 is not shown because it is similar to AF660.

Received: November 27, 2013
Published: February 25, 2014

dx.doi.org/10.1021/ja411843k | *J. Am. Chem. Soc.* 2014, 136, 4599−4604

Table 1. Fitting Parameters for Lifetime Data

sample		τ1 ns (amplitude %)	τ2 ns (amplitude %)	τ3 ns (amplitude %)	average lifetime (ns)[a]	quantum yield[b]
AF647 λ_{ex} = 600 nm	free	0.41 (6.9)	1.09 (93.1)	–	1.04	0.33
	BSA	0.05 (30.8)	0.64 (19.8)	1.73 (49.4)	0.99	0.43
	RC	0.07 (62.9)	0.46 (16.2)	1.61 (20.9)	0.45	–
AF660 λ_{ex} = 600 nm	free	0.55 (19)	1.24 (81)	–	1.11	0.37
	BSA	0.10 (13.2)	0.81 (25.5)	1.82 (61.3)	1.33	0.32
	RC	0.04 (67.9)	0.31 (16.1)	1.46 (16.0)	0.31	–
	Q^-RC	0.05 (60.3)	0.47 (18.9)	1.60 (20.8)	0.45	–
AF750 λ_{ex} = 710 nm	free	0.55 (98.6)	1.17 (1.4)	–	0.56	0.12
	BSA	0.12 (11.7)	0.73 (76.0)	1.63 (12.3)	0.77	0.12
	RC	0.06 (40.0)	0.38 (34.6)	0.85 (25.4)	0.37	–

[a]Average lifetime is calculated as $\tau_{ave} = \sum_i A_i\tau_i/\sum_i A_i$, where A_i and τ_i are the amplitude and the lifetime components. [b]Quantum yield of fluorescence is calculated as $\Phi = \Phi_R\ IA_R\eta^2/I_RA\eta_R^2$, where Φ and Φ_R are the quantum yield of the sample and the reference, I and I_R are the fluorescence intensities of sample and reference, A and A_R are the absorbance of sample and reference at the excitation wavelength, η and η_R are the refractive indexes of solvents for sample and reference, respectively.

develop a geometrically defined system for systematically studying the effects of pigment spectrum, attachment point, and fluorescence lifetime on the energy-transfer efficiency to the reaction center. This study should help define some of the parameters important for designing novel molecular photonic devices.

RESULTS AND DISCUSSION

For these studies, a mutant of the *Rhodobacter sphaeroides* 2.4.1 RC (PDB 2J8C) is used that contains three specific and unique cysteine residues near the primary electron donor, P. These Cys residues have been conjugated to several commercially available fluorescent dye molecules with different spectral properties. Using this system, the interplay between absorbance cross-section, spectral breadth of light harvesting, excited-state lifetime, and energy-transfer efficiency can be explored.

The structure of the RC complex is shown in Figure 1A, which consists of three polypeptide subunits H, M, and L. The L and M subunits are associated with 10 cofactors: a dimer of bacteriochlorophylls (P), two bacteriochlorophylls (B_A and B_B), two bacteriopheophytins (H_A and H_B), two molecules of ubiquinone-10 (Q_A and Q_B), one carotenoid, and one nonheme iron atom (Fe^{2+}).[4] P is the primary electron donor, and upon excitation, it transfers an electron to Q_A via B_A and H_A, forming a long-lived charge-separated state $P^+Q_A^-$. Eventually electron transfer occurs from the reduced primary quinone to the secondary quinone Q_B forming $P^+Q_B^-$. There are three distinct spectral bands between 700 and 900 nm in the RC absorption spectrum (Figure 1B, black curve), which predominantly represent H_A and H_B (760 nm), B_A and B_B (804 nm), and P (860 nm), respectively.[5]

The genetically modified RC protein used in this study contains three Cys residues (M100C, L72C and L274C) located on the surface of the M and L subunits, respectively, close to P. All the other Cys residues were replaced with either serine or alanine.[6] Fluorophores were covalently conjugated to these three surface Cys residues via reactive maleimide groups (for details of the sample preparation, purification, and characterization see Supporting Information). The cysteines are situated more than 3.5 nm from one another to avoid the possibility of intramolecular disulfide bond formation and also to prevent direct interactions between the attached fluorophores. The distances between each Cys and P range from 3.0 to 3.7 nm. By selecting different dye molecules the overall absorption cross section of the assembled system can be tuned over a broad range (Figure 1B).[7]

The three dye molecules used in this study are Alexa Fluor 647 (AF647, $\lambda_{max,abs}$ = 649 nm, $\lambda_{max,em}$ = 667 nm, fluorescence quantum yield = 0.33), Alexa Fluor 660 (AF660, $\lambda_{max,abs}$ = 660 nm, $\lambda_{max,em}$ = 690 nm, fluorescence quantum yield = 0.37), and Alexa Fluor 750 (AF750, $\lambda_{max,abs}$ = 752 nm, $\lambda_{max,em}$ = 780 nm, fluorescence quantum yield = 0.12). The fluorophores were chosen in such a way that they substantially increase the absorbance cross section in the spectral regions where the absorbance of the RC is low, and there is significant spectral overlap between the emission spectra of the dye and the absorbance of the RC pigments.

To better understand the spectral and kinetic properties of the Alexa Fluor dyes in a protein environment without an energy acceptor, the dye molecules were conjugated to a spectrally inactive protein, bovine serum albumin (BSA), using the same maleimide chemistry used for RC-dye conjugation. These samples were used as controls in the spectroscopic measurements. A 4 nm red-shift in the absorbance and a 7 nm red-shift in the fluorescence of the AF660 dye were observed when it was attached to a surface-exposed Cys of BSA (average dye/BSA ratio 0.8), compared to the free dye in solution. Similar spectral shifts were observed for BSA-AF647 conjugates (average dye/BSA ratio 0.8) and BSA-AF750 conjugates (average dye/BSA ratio 0.6) (Figures S2–S4). The shift apparently reflects the influence of the protein environment on the spectral properties of the dye molecules. A comparison between fluorescence quantum yield of free dye and the BSA conjugated dyes is shown in Table 1.

The three dyes (AF647, AF660 and AF750) were conjugated separately to the RC that resulted with dye-to-RC ratios of 2.5, 2.6, and 2.2, respectively. The covalent conjugation of AF660 to the RC was confirmed by matrix-assisted laser desorption ionization time-of-flight (MALDI-TOF) mass spectrometry using α-cyano-4-hydroxycinnamic acid as matrix.[3a,8] The RC shows three distinct peaks corresponding to its three protein subunits (H, L, and M), whereas the RC-AF660 conjugate exhibits two additional peaks associated with the L-subunit and one additional peak associated with the M-subunit, each with a 840–920 Da mass shift. This result confirms that the conjugation of the dye molecule to the RC protein was selective and site-specific (Figures 2B and S1).

The absorption spectrum of the dye-conjugated RC shows strong absorbance between 550 and 750 nm, where the RC

dx.doi.org/10.1021/ja411843k | J. Am. Chem. Soc. 2014, 136, 4599–4604

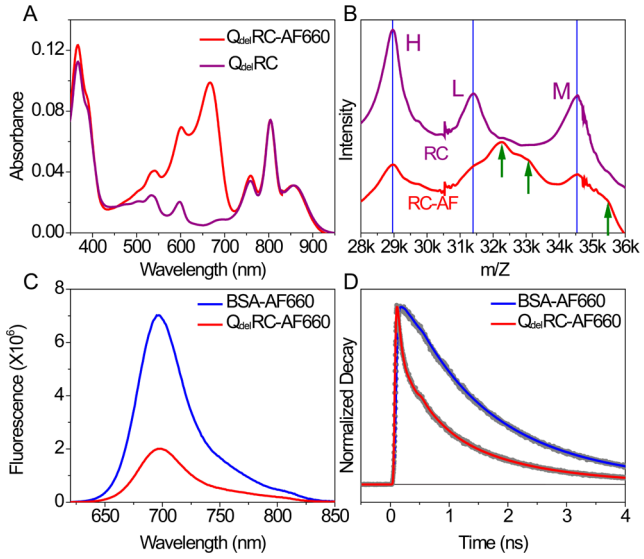

Figure 2. (A) Absorption spectra of quinone-depleted RCs (Q_{del}RC, purple) and AF660 conjugated quinone-depleted RCs with dye to RC ratio of 2.5 (Q_{del}RC-AF660, red). (B) MALDI-TOF spectra of RC (purple) and AF660 conjugated RC (red). The RC spectrum shows three peaks corresponding to H, L, and M subunits, whereas the RC-AF spectrum has two and one extra peaks for L and M, respectively, signifying selective and site-specific conjugation of the dye to the RC. (C) Fluorescence emission spectra of AF660 conjugated to BSA (blue) and quinone-depleted RC (red) with excitation at 600 nm. The spectra were corrected by detector response file and scaled by the dye absorbance at 600 nm. A 70% fluorescence intensity decrease is observed likely due to energy transfer from AF660 to quinone-depleted RC. (D) Fluorescence lifetime decay traces of AF660 conjugated to BSA (blue) and quinone-depleted RC (red) monitored at 698 nm (λ_{ex} = 600 nm).

itself absorbs only weakly (Figures 2A and S2−S5). There is a 4 nm shift in the absorbance and a 7 nm shift in the fluorescence of the AF660 dye when attached to the RC, compared to the free dye in solution, similar to that of the BSA-AF660 conjugate. The same trends were also observed for the RC-AF647 and RC-AF750 conjugates. For this reason, the BSA-dye conjugates were used as reference samples, rather than the free dyes in solution, for all spectroscopic measurements.

For some experiments, both quinones (Q_A and Q_B) were removed from the RC, so that the charge-separated state ($P^+H_A^-$) recombines to the ground state in nanoseconds, to ensure a complete recovery of P before each laser excitation in transient absorbance measurements (see Supporting Information for details).[9] AF660 conjugated to the quinone-depleted RC had an average dye-to-RC ratio of 2.5 and has essentially the same absorbance spectrum as the quinone-containing, AF660-conjugated RCs.

When the quinone-depleted RC-AF660 conjugate was excited at 600 nm, the relative steady-state fluorescence intensity from the AF660 dye was much reduced compared to that of the BSA-AF660 conjugate with the same dye absorbance (~70% fluorescence quenching), as would be expected if there were substantial energy transfer from the dye to the RC pigments. The corresponding quenching of the fluorescence emission was found to be 59% and 60% for the RC-AF647 and RC-AF750 conjugates, respectively, compared to the corresponding BSA-conjugated controls. Although the fluorescence emission spectrum of AF750 overlaps better with the RC absorption between 700 and 900 nm than does the spectrum of AF660, the RC-AF660 conjugate has higher energy-transfer efficiency.

Time-resolved fluorescence decay measurements of the various free dyes, BSA- and RC-dye conjugates were performed using time-correlated single-photon counting techniques. Kinetic analysis of all free dyes in solution revealed a biexponential decay (Table 1, Figure S6). The amplitude-weighted average lifetimes of each dye are 1.04 ns for AF647, 1.11 ns for AF660, and 0.56 ns for AF750. In contrast, exponential fitting of the fluorescence decay kinetics for each of the protein-dye molecule conjugates required three exponential components (Table 1). The average lifetimes for the BSA-conjugated dyes were comparable to or slightly longer than the free dyes in solution (0.99, 1.33, and 0.77 ns for BSA-AF647, -AF660 and -AF750, respectively). The increase in the complexity seen in the fluorescence decay of the dye conjugated on the protein surface compared to the free dye is not surprising. As can be seen from the quantum yields of fluorescence (Table 1), the decay lifetime is dominated by nonradiative pathways (vibrational coupling between the ground and excited states). The vibrational manifold of the protein environment is more complex than that of a homogeneous solvent. The shift in the environment in the BSA-conjugates compared to the free dyes also gives rise to the small red-shift alluded to previously in the peak absorbance and emission spectra of the dyes upon conjugation (Figures 2A and S2−S5), presumably due to an overall change in polarity or polarizability of the environment.

A substantial decrease in the average fluorescence decay lifetime of each dye is observed in the RC-dye conjugates; lifetimes of 0.45, 0.45, and 0.37 ns were measured for the RC-AF647 conjugate, the quinone-depleted RC-AF660 conjugate, and the RC-AF750 conjugate, respectively. For the RC-AF647 and RC-AF660 conjugates, the decrease in the average lifetime is primarily due to an increase in the amplitude of the shortest (~50 ps) decay component (Tables 1 and S2). For AF750, the lifetimes of all three components in the decay decreased. The overall decrease in average fluorescence lifetime (dye excited-state lifetime) is consistent with a substantial level of energy transfer from the dye to the reaction center cofactors. Again, the complexity of the decay in the reaction center conjugates is likely due to the heterogeneity of the local environment (static or dynamic) and its effects on both energy transfer (which is sensitive to transition dipole orientation of the donor and acceptor) and nonradiative decay via vibrational coupling to the ground state.

A comparison of the average lifetimes for the dye conjugated to the RC vs the dye conjugated to BSA resulted in estimated energy-transfer quantum yields of 55%, 66%, and 52%, for RC-AF647, quinone-depleted RC-AF660, and RC-AF750, respectively, which is in reasonable agreement with the results obtained from steady-state fluorescence (59%, 70%, and 60%, respectively, see also Table S4). Thus, in either time-resolved or steady-state fluorescence measurements, higher energy-transfer efficiency is observed for the RC-AF660 conjugates compared to the RC-AF750 conjugates, even though the fluorescence spectrum of AF750 shows a larger overlap with the absorbance spectrum of the RC pigments than does the fluorescence spectrum of AF660. In the time domain, one can directly see that the AF660 dye has a longer intrinsic excited-state lifetime than does the AF750 dye, corresponding to its high fluorescence quantum yield (Table 1). Thus there is more opportunity for the excited state of AF660 to transfer energy to

dx.doi.org/10.1021/ja411843k | J. Am. Chem. Soc. 2014, 136, 4599−4604

P. This exemplifies the key role of donor excited-state lifetime in the design of light-harvesting systems.

One would expect that energy transfer from a dye to RC pigments would lead to charge separation. Because charge separation in the RC occurs with near unity yield, the amount of charge separation that takes place should track the energy-transfer efficiency. The relative amount of RC charge separation was determined by comparing the light-minus-dark difference spectrum (the degree of ground-state bleaching of the P band at 865 nm) of the RC-AF660 conjugate with that of unconjugated RCs. Each sample was illuminated through a band-pass filter centered at 650 nm (bandwidth 10 nm). The light intensities used were low enough so that all signals increased linearly with intensity, ensuring that the amplitude of the P-band bleaching measured at 865 nm reflects the relative amount of the $P^+Q_A^-$ formed in each sample. As shown in Figure 3, $P^+Q_A^-$ in the unconjugated RCs shows an absorbance

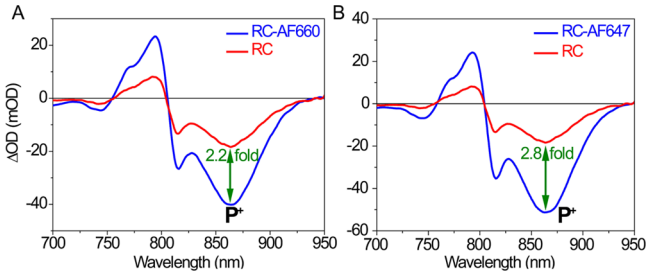

Figure 3. (A) Light-minus-dark absorbance spectra of RC-AF660 (blue) and unconjugated RCs (red). A 2.2-fold enhancement in P^+ formation is observed due to the enhanced absorption cross-section at 650 nm. (B) RC-AF647 shows a 2.8-fold enhancement in P^+ formation over unconjugated RCs.

difference spectrum that involves negative and positive signals at 865 and 770 nm, respectively. The RC-AF660 conjugates show essentially the same absorbance change but 2.2-fold greater in magnitude than that of the unconjugated RCs, showing that the energy of the 650 nm photons absorbed by AF660 and transferred to the RC cofactors is effective in charge-separated state formation (most of the 650 nm light absorbed by the RC-AF660 conjugates is absorbed by the dye, as shown in Figure 1B). Similarly, the AF647 conjugated RCs show a 2.8-fold enhancement in P^+ formation over unconjugated RCs excited at 650 nm. The increase in enhancement corresponds to the higher absorption cross section at 650 nm of RC-AF647 compared to that of RC-AF660 (See Figure S8 for absorption data).

All of the processes, from excitation of the dye to charge separation in the RC, can be observed kinetically via transient absorbance spectroscopy. Absorbance difference spectra as a function of time for both the AF660 dye (650–750 nm) and the initial electron donor, P, in the RC (800–940 nm with the peak at 860 nm) were monitored over a broad wavelength region at different time delays following excitation at 650 nm. At this excitation wavelength, the AF660 dye contributes more than 95% of the sample absorbance.

The transient absorbance difference spectra induced by the bleaching of AF660 and P in the quinone-depleted RC-AF660 conjugates, recorded at various delay times, were compared with those of both the free dye and of unconjugated, quinone-depleted RCs (Figure 4). For the quinone-depleted RC-AF660 conjugates, the ground-state bleaching signal in the 650–750

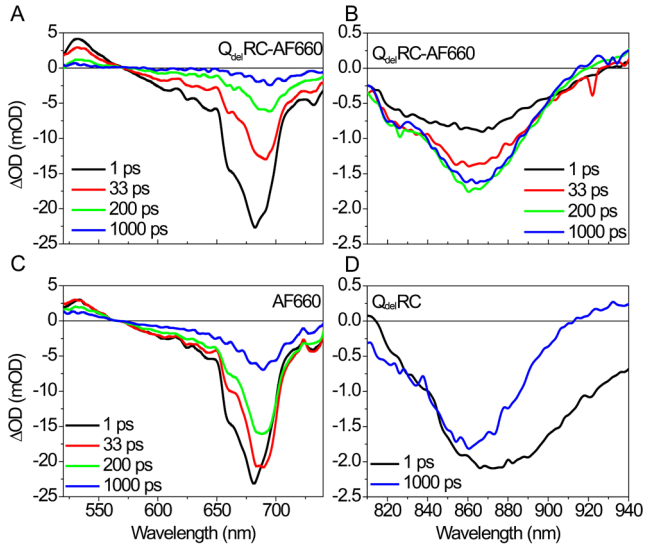

Figure 4. (A) Time-resolved transient absorption difference spectra of quinone-depleted RC-AF660 conjugates in the 530–730 nm region and (C) AF660 dye itself in solution. (B) Time-resolved transient absorption difference spectra of quinone-depleted RC-AF660 conjugates and (D) unconjugated quinone-depleted RCs in the 800–940 nm region (near the maximal ground-state absorbance of the RC cofactor P). For all samples, λ_{ex} = 650 nm.

nm region appeared instantaneously and then recovered by about 80% during the first 200 ps (Figure 4A), indicating the disappearance of the excited-state population of AF660. As the AF660 ground-state absorbance recovered, an absorbance decrease associated with bleaching of the ground-state spectrum of P developed in the 800–940 nm region (Figure 4B). In quinone-depleted RCs, the terminal charge-separated state is $P^+H_A^-$, which forms within a few ps[5a,10–12] but then lives for 10–20 ns.[5a,13] Thus, once formed, the bleaching of the ground-state absorbance from P remains constant on the time scale of this measurement.

In contrast to the situation in quinone-depleted RC-AF660 conjugates, the ground-state bleaching that is generated upon excitation of the unconjugated AF660 dye itself does not decay very much during the initial 200 ps (Figure 4C). Instead, the dye bleaching decreases over a roughly 1 ns time period, consistent with its inherent excited-state lifetime (Table 1). Similar results have been observed for the BSA-AF660 construct (Figure S9A). As a control, transient absorption spectra of quinone-depleted RCs without dye were recorded at two different delay times, when the RCs are dominated by the state P* (1 ps) and the state $P^+H_A^-$ (1 ns), again excited at 650 nm (Figure 4D). Although the absorbance at 650 nm is weak in unconjugated RCs, some RCs are excited. As expected, the spectrum at 1 ns has the same profile as that obtained from the dye-conjugated RC, consistent with formation of the long-lived charge-separated state $P^+H_A^-$ in both samples. However, the spectrum of unconjugated, quinone-depleted RCs at 1 ps shows spectral changes expected for the direct excitation of the RC, forming the excited state of P (P*) rather than the absorbance changes associated with the excited state of the dye, as seen in the dye conjugated RCs. The P* signal consists of a large absorbance extending between the 860 nm region (ground-state bleaching) and the 900 nm region (stimulated emission from P*). The lack of stimulated emission signal in the quinone-depleted RC-AF660 conjugates (Figure 4B) is due to

dx.doi.org/10.1021/ja411843k | J. Am. Chem. Soc. 2014, 136, 4599–4604

the low steady-state population of P*; energy transfer forming P* from AF660 takes place in tens of ps, whereas the conversion of P* to P^+ takes only 3 ps.[5a]

The ground-state bleaching of the dye absorbance following a pulse directly exciting the dye (at 650 nm) should recover as the dye excited-state decays. The dye ground-state recovery kinetics was compared for the unconjugated AF660 dye and the quinone-depleted RC-AF660 conjugates (Figure 5A), probing

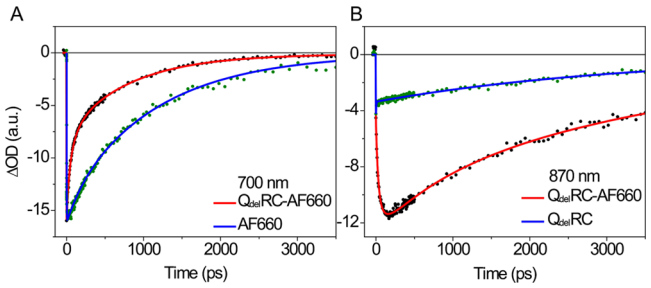

Figure 5. Transient absorbance kinetics (A) at 700 nm for unconjugated AF660 dye in solution (AF660, blue) and quinone-depleted RC-AF660 conjugates (Q_{del}RC-AF660, red). (B) Ground-state bleaching of P at 870 nm in unconjugated RCs (Q_{del}RC, blue) and quinone-depleted RC-AF660 conjugates (Q_{del}RC-AF660, red). Excitation is at 650 nm.

at 700 nm. In agreement with the single photon counting measurements (Figure 2D) and the conclusions drawn from analysis of the time-resolved spectra in Figure 4, the excited-state lifetime of the AF660 in quinone-depleted RC-AF660 conjugates is much shorter than that of the free dye in solution, again supporting the conclusion that energy transfer is the dominant pathway of dye excited-state decay in the RCs conjugated to dye. The absorbance change kinetics were fit with three exponential components. The fastest lifetime resulting from the fit was 25 ps. This is shorter than the ~50 ps lifetime obtained from multiexponential fits of the single photon counting data, likely due to the higher time resolution of the transient absorbance measurements (0.1 ps vs 40 ps). An average lifetime of 570 ps (25 ps (35%), 164 ps (29%), and 1418 ps (36%)) over the whole decay was determined for quinone-depleted RC-AF660 conjugates from transient absorbance measurements, while AF660 in solution gave an average lifetime of 1130 ps (519 ps (30%) and 1390 ps (70%)) (Table S3). For comparison, the average lifetime of the BSA-AF660 conjugate used as a control was 1570 ps (531 ps (18%) and 1800 ps (82%)). A comparison of the average lifetimes for the dye conjugated to the RC vs the dye conjugated to BSA resulted in an estimate of 64% for the overall energy-transfer efficiency (Table S4), which is in reasonable agreement with the results obtained from steady-state fluorescence (70%) and time correlated single photon counting measurements (66%).

The relative amounts of P^+ formed in RCs with and without AF660 conjugated were determined by comparing the extent of ground-state bleaching at 870 nm (Figure 5B). Using excitation at 650 nm, where the unconjugated RC absorbs weakly, roughly a 2.7-fold increase in P^+ formation was observed in the quinone-depleted RC-AF660 conjugate compared to the unconjugated, quinone-depleted RC at the same concentration, in agreement with the results of steady-state $P^+Q_A^-$ formation monitored via light-minus-dark difference spectroscopy (Figure 3).

If energy transferred from the AF660 dye to P results in P^+ formation, one would expect that the kinetics of AF660 ground-state recovery (700 nm) would match that of the formation of ground-state bleaching due to formation of P^+ (870 nm). As shown in Figure S7, this is indeed the case; the normalized traces show a fast decay of the dye and a concomitant formation of the P^+ signal. The kinetic trace from unconjugated RC is shown for comparison and exhibits instantaneous formation of the P bleaching signal due to the direct excitation of RC cofactors.

A key aspect of natural RC function is the ability to accept electrons from soluble cytochrome *c*. Given the proximity of the conjugated dye molecules to the cytochrome binding site, one might think that dye would interfere with cytochrome binding and thus electron transfer to P^+. To explore this possibility further, cytochrome *c* was added to a solution of dye-conjugated RCs, and the absorbance changes associated with cytochrome *c* oxidation were monitored at 550 nm.[3a,14] The RC-AF647 and RC-AF660 conjugates were able to oxidize soluble cytochrome *c* much more rapidly than unconjugated RCs when 650 nm excitation was used (Figure 6). In fact, the

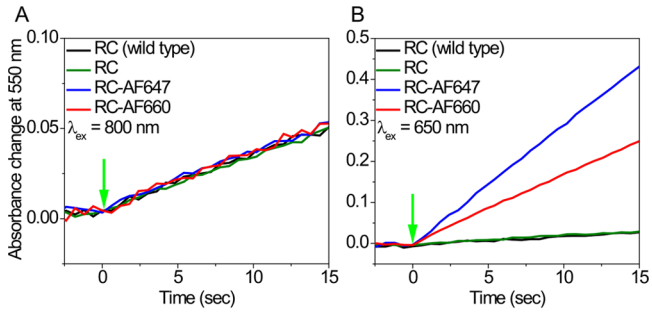

Figure 6. Cytochrome *c* oxidation was monitored at 550 nm after 800 nm (A) and 650 nm (B) excitation. At 800 nm excitation, each of the samples shows similar kinetics, whereas using 650 nm excitation, the dye conjugated samples display much faster rates of cytochrome *c* oxidation compared to the wild-type (RC wild-type) and cysteine mutated (RC) RCs. RC-AF647 has a faster rate than that of RC-AF660 due to its higher absorption cross-section at 650 nm. The absorbance change scales are different because the light intensities at 650 and 800 nm are not the same.

increase in the rate of cytochrome *c* oxidation observed using 650 nm excitation was at least as large as the increase in $P^+Q_A^-$ formation seen in the light-minus-dark spectral measurements (Figure 3), consistent with an increase in absorbance cross section at 650 nm and implying that the presence of the dye molecules did not substantially inhibit electron transfer to the cytochrome. As expected, dye conjugated and unconjugated samples showed a similar rate of cytochrome *c* oxidation using 800 nm excitation where all the samples have same absorption cross section.

CONCLUSION

Conjugation of any of the three dyes tested at positions near P in the RC results in a substantial increase in the effective absorbance cross section for charge separation in the visible part of the spectrum where the dyes absorb strongly, but the RC has weak absorbance. Further, it was possible to specifically place the dye molecules at positions that were well within the Förster energy-transfer distance to P and yet did not substantially perturb the ability of P to either donate electrons

dx.doi.org/10.1021/ja411843k | J. Am. Chem. Soc. 2014, 136, 4599−4604

to subsequence cofactors in the normal electron-transfer sequence or to accept electrons from soluble cytochrome *c*.

The ability to functionally couple any of several different dyes to the RC makes it possible to tune the action spectrum of the system over a broad range. This type of model system also makes it possible to start defining the parameters involved in the design and construction of more complex molecular photonic devices, such as the effects of geometry, dye environment, dye excited-state lifetime, and the type and conformational flexibility of dye conjugation chemistry.

■ ASSOCIATED CONTENT

Supporting Information

Methods and additional data. This material is available free of charge via the Internet at http://pubs.acs.org.

■ AUTHOR INFORMATION

Corresponding Authors

Hao.Yan@asu.edu
nwoodbury@asu.edu

Notes

The authors declare no competing financial interest.

■ ACKNOWLEDGMENTS

We thank Chad Lunceford and Brent Driscoll for their help in setting up the spectroscopy for light-minus-dark experiment. This research was supported by Multidisciplinary University Research Initiative (MURI) program (award W911NF-12−1−0420) funded by Army Research Office (ARO) to H.Y. and N.W. and a grant from the Canadian Natural Sciences and Engineering Research Council to J.T.B.

■ REFERENCES

(1) (a) Blankenship, R. E. *Molecular Mechanisms of Photosynthesis*; Blackwell Science: Oxford, 2002. (b) Scholes, G. D.; Fleming, G. R.; Olaya-Castro, A.; van Grondelle, R. *Nat. Chem.* **2011**, *3*, 763. (c) McDermott, G.; Prince, S. M.; Freer, A. A.; Hawthornthwaite-Lawless, A. M.; Papiz, M. Z.; Cogdell, R. J.; Isaacs, N. W. *Nature* **1995**, *374*, 517. (d) Wraight, C. A.; Clayton, R. K. *Biochim. Biophys. Acta* **1974**, *333*, 246.

(2) Nabiev, I.; Rakovich, A.; Sukhanova, A.; Lukashev, E.; Zagidullin, V.; Pachenko, V.; Rakovich, Y. P.; Donegan, J. F.; Rubin, A. B.; Govorov, A. O. *Angew. Chem., Int. Ed.* **2010**, *49*, 7217.

(3) (a) Milano, F.; Tangorra, R. R.; Omar, O. H.; Ragni, R.; Operamolla, A.; Agostiano, A.; Farinola, G. M.; Trotta, M. *Angew. Chem., Int. Ed.* **2012**, *51*, 11019. (b) Boxer, S. G.; Stocker, J.; Franzen, S.; Salafsky, J. *AIP Conf. Proc.* **1992**, *262*, 226. (c) Salafsky, J.; Groves, J. T.; Boxer, S. G. *Biochemistry* **1996**, *35*, 14773.

(4) (a) Allen, J. P.; Feher, G.; Yeates, T. O.; Komiya, H.; Rees, D. C. *Proc. Natl. Acad. Sci. U.S.A.* **1987**, *84*, 6162. (b) Feher, G.; Allen, J. P.; Okamura, M. Y.; Rees, D. C. *Nature* **1989**, *339*, 111. (c) Jones, M. R. *Prog. Lipid Res.* **2007**, *46*, 56.

(5) (a) Kirmaier, C.; Holten, D. *Photosynth. Res.* **1987**, *13*, 225. (b) Woodbury, N. W.; Allen, J. P. The Pathway, Kinetics and Thermodynamics of Electron Transfer in the Reaction Centers of Purple Nonsulfer Bacteria. In *Anoxygenic Photosynthetic Bacteria*; Blankenship, R. E., Madigan, M., Bauer, C. E., Eds.; Kluwer Academic Publishers: Netherlands, 1995; p 527. (c) Kirmaier, C.; Laporte, L.; Schenck, C. C.; Holten, D. *J. Phys. Chem.* **1995**, *99*, 8903. (d) Zinth, W.; Wachtveitl, J. *ChemPhysChem* **2005**, *6*, 871. (e) Parson, W. W.; Warchel. A. Mechanism of Charge Separation in Purple bacterial Reaction centers. In *The Purple Phototrophic Bacteria*; Hunter, C. N., Daldal, F., Thurnauer, M. C., Beatty, J. T., Eds.; Springer: Netherlands, 2009; p 355.

(6) Mahmoudzadeh, A.; Saer, R.; Jun, D.; Mirvakili, S. M.; Takshi, A.; Iranpour, B.; Ouellet, E.; Lagally, E. T.; Madden, J. D. W.; Beatty, J. T. *Smart Mater. Struct.* **2011**, *20* (9), 094019.

(7) Dutta, P. K.; Varghese, R.; Nangreave, J.; Lin, S.; Yan, H.; Liu, Y. *J. Am. Chem. Soc.* **2011**, *133*, 11985.

(8) (a) Cadene, M.; Chait, B. T. *Anal. Chem.* **2000**, *72*, 5655. (b) Gabant, G.; Cadene, M. *Methods* **2008**, *46*, 54.

(9) Lin, S.; Xiao, W.; Eastman, J. E.; Taguchi, A. K. W.; Woodbury, N. W. *Biochemistry* **1996**, *35*, 3187.

(10) Holzwarth, A. R.; Müller, M. G. *Biochemistry* **1996**, *35*, 11820.

(11) Huppman, P.; Arlt, T.; Penzkofer, H.; Schmidt, S.; Bibikova, M.; Dohse, B.; Oesterhelt, D.; Wachtveit, J.; Zinth, W. *Biophys. J.* **2002**, *82*, 3186.

(12) Van Stokkum, I. H. M.; Beekman, L. M. P.; Jones, M. R.; Van Brederode, M. E.; Van Grondelle, R. *Biochemistry* **1997**, *36*, 11360.

(13) Chidsey, C. E. D.; Kirmaier, C.; Holten, D.; Boxer, S. G. *Biochim. Biophys. Acta* **1984**, *766*, 424.

(14) Gerencsér, L.; Laczkó, G.; Maróti, P. *Biochemistry* **1999**, *38*, 16866.